CHAPTER 150

TSUNAMI GENERATION AND PROPAGATION

by

Joseph L. Hammack, Jr.[1] and Fredric Raichlen[2]

ABSTRACT

A linear theory is presented for waves generated by an arbitrary bed deformation (in space and time) for a two-dimensional and a three-dimensional fluid domain of uniform depth. The resulting wave profile near the source is computed for both the two and three-dimensional models for a specific class of bed deformations; experimental results are presented for the two-dimensional model.

The growth of nonlinear effects during wave propagation in an ocean of uniform depth and the corresponding limitations of the linear theory are investigated. A strategy is presented for determining wave behavior at large distances from the source where linear and nonlinear effects are of equal magnitude. The strategy is based on a matching technique which employs the linear theory in its region of applicability and an equation similar to that of Korteweg and deVries (KdV) in the region where nonlinearities are equal in magnitude to frequency dispersion. Comparison of the theoretical computations with the experimental results indicates that an equation of the KdV type is the proper model of wave behavior at large distances from the source region.

INTRODUCTION

The main body of tsunami research has originated in Japan as a natural consequence of the devastating effects of tsunamis on this nation. In early investigations of tsunami generation, e.g., Takahasi (1942, 1945, 1947), Ichiye (1950), Honda and Nakamura (1951), Nakamura (1953) integral expressions (based on a linear theory) were developed to describe the waves resulting from various bed deformations in both two and three-dimensional fluid domains. The difficulty in evaluating these complex expressions for the generated waves precluded a detailed understanding of their character. Webb (1962) and Momoi (1964) developed the wave profiles near the disturbance using high-speed computational facilities. (It should be noted that the bed deformation adopted by Webb is of special interest since it is also one of the models investigated in this study; it appears that an error was made in the earlier solution by Webb.) The waves at large distance from the source region (and at large times after generation) have been investigated by several authors including Keller (1963) and Kajuira (1963) using asymptotic methods such as the method of stationary phase. More recently Hwang and Divoky (1970) have developed a numerical model of tsunami generation based on the shallow-water-wave equations; this model has been applied to the Alaskan earthquake of 1964. The only experimental investigations of tsunami generation (using bed deformations to generate the waves) appears to be those of Takahasi (1963) and Takahasi and Hatori (1962).

[1] Research Fellow in Civil Engineering, W. M. Keck Laboratory of Hydraulics and Water Resources, California Institute of Technology, Pasadena, California, U.S.A.

[2] Professor of Civil Engineering, W. M. Keck Laboratory of Hydraulics and Water Resources, California Institute of Technology, Pasadena, California, U.S.A.

Although numerous authors have investigated the tsunami problem, none appear to have thoroughly studied the wave profiles generated over a full range of characteristic size and time scales for a specific bed deformation. In addition, no authors appear to have determined the restrictions on the applicability of the linearized description of wave behavior for generating and propagating a wave. In this investigation a linear theory has been adopted to describe the waves; however, the effects of nonlinearities during generation and propagation will be examined (for the two-dimensional model). A three-dimensional model of tsunami generation will be discussed, based on a linear theory, and differences between the results for the two and three-dimensional models near the region of generation will be examined. Experiments have been conducted in a wave tank equipped with a section of the bottom which can be moved in a programmed fashion by an hydraulic-servo-system, and these results are compared to the two-dimensional theory.

THEORETICAL ANALYSIS

Consider a fluid domain D as shown in Fig. 1 bounded above by the free surface, S_f, below by the solid boundary, S_b, and unbounded in the direction of wave propagation, i.e., $-\infty < x < \infty$. Initially the fluid is at rest, with the free

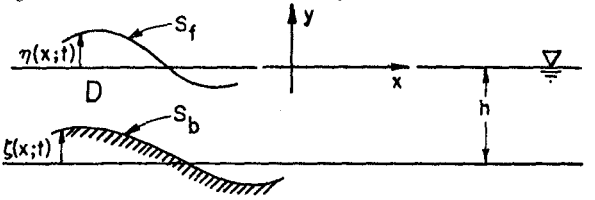

Fig. 1. Definition sketch of coordinate system.

surface and the solid boundary defined by y = 0 and y = -h, respectively. For t > 0 the bed (or solid boundary) is permitted to move in a prescribed manner given by $y = -h + \zeta(x;t)$ such that $\lim_{|x|\to\infty} \zeta(x;t) = 0$. The resulting deformation of the free surface, which is to be determined, is given by $y = \eta(x;t)$. Assuming the fluid to be incompressible and the flow irrotational, a velocity potential $\varphi(x, y;t)$ is known to exist such that $\vec{q} = \nabla\varphi$ where $\vec{q}$ is the velocity vector, i.e., $\vec{q} = (u, v)$. From the continuity equation $\nabla \cdot \vec{q} = 0$, it is found that:

$$\nabla^2\varphi = 0 \text{ in D.} \tag{1}$$

The kinematic conditions to be satisfied on the free surface and on the solid boundary are:

$$\varphi_y = \eta_t + \varphi_x\eta_x \qquad \text{on } y = \eta(x;t), \tag{2}$$

$$\varphi_y = \zeta_t + \varphi_x\zeta_x \qquad \text{on } y = -h + \zeta(x;t) \tag{3}$$

By further assuming the flow to be inviscid and surface energy effects to be negligible the dynamic condition to be satisfied by the fluid particles on the free surface becomes:

$$\varphi_t + \tfrac{1}{2}(\nabla\varphi)^2 + g\eta = 0 , \tag{4}$$

where the pressure on the free surface has been taken as zero.

Solution of Eqs. (1), (2), (3), and (4) is inherently difficult due to the nonlinear terms in the boundary conditions and the unknown location of the free surface on which the boundary conditions are to be applied. These difficulties can be circumvented by assuming the effects of the nonlinear terms to be small relative to the linear effects and applying the linearized boundary conditions at the original positions of the fluid boundaries. The linearized boundary conditions are given by:

$$\varphi_{tt}(x, 0;t) + g\varphi_y(x, 0;t) = 0 , \tag{5}$$

$$\varphi_y(x, -h;t) = \zeta_t(x;t) , \tag{6}$$

where the kinematic and dynamic conditions on the free surface have been combined into a single condition given by Eq. (5). The requirements necessary for this linearized approximation to provide an accurate description of the fluid behavior will be discussed in more detail shortly.

The solution of Eqs. (1), (5), and (6) for the previously stated initial conditions and an arbitrary bed displacement has been presented in detail by Hammack (1972). Using the Fourier transform with respect to the x-coordinate and the Laplace transform with respect to time, t, the water surface displacement was found to be:

$$\eta(x;t) = \frac{1}{2\pi}\int_{-\infty}^{\infty} e^{-ikx}\left\{\lim_{\Gamma\to\infty}\frac{1}{2\pi i}\int_{\mu-i\Gamma}^{\mu+i\Gamma}\frac{s^2 e^{st}\overline{\zeta}(k;s)}{(s^2+\omega^2)\cosh kh}\,ds\right\}dk , \tag{7}$$

where:
$$\omega^2 \equiv gk \tanh kh , \tag{8}$$

$$\overline{\zeta}(k;s) = \int_{-\infty}^{\infty} dx \int_0^{\infty} e^{ikx} e^{-st}\zeta(x;t)\,dt . \tag{9}$$

The bracketed quantity in Eq. (7) is the complex inversion integral for the Laplace transform; the remaining integration represents the inversion integral for the Fourier transform.

A specific bed deformation, $\zeta(x;t)$, must be prescribed before Eq. (7) can be simplified further. Of special interest in the present study is a bed deformation described mathematically by:

$$\zeta_e(x,t) = \zeta_o(1-e^{-\alpha t})\,H(b^2-x^2) \qquad \text{for } t > 0 , \tag{10}$$

where H( ) is the Heavyside step function. Eq. (10) indicates that a block section of the bed, symmetric about x = 0 with a length of 2b, moves in an asymptotic manner to an elevation of ζ_o which may be either above or below the initial bed location. This bed deformation can be characterized by three parameters: an amplitude, ζ_o, a size, b, and a characteristic time, t_c. For convenience the characteristic time which has been chosen is the time required for two-thirds of the movement to be completed, i.e., $t = t_c$ when $\zeta/\zeta_o = 2/3$ or $t_c = 1.11/\alpha$. This bed deformation will hereafter be referred to as the exponential bed motion.

Before Eq. (7) can be simplified, the bed motion, $\zeta_e(x;t)$, must be transformed by Eq. (9); performing these integrations yield:

$$\overline{\zeta}_e(k;s) = 2\zeta_o\frac{\sin kb}{k}\left[\frac{\alpha}{s(s+\alpha)}\right] . \tag{11}$$

Substituting Eq. (11) into Eq. (7), performing the integration around the Bromwich contour in the complex s-plane, taking only the real part of the results, and noting that the integrand is an even function of k yields:

$$\eta(x;t) = -\frac{2\zeta_o}{\pi}\int_0^\infty \frac{\cos kx \sin kb}{k \cosh kh}\left(\frac{\alpha^2}{\alpha^2+\omega^2}\right)\left[e^{-\alpha t} - \cos \omega t - \frac{\omega}{\alpha}\sin \omega t\right] dk \ . \qquad (12)$$

Eq. (12) represents the water surface movement resulting from the exponential bed displacement in a two-dimensional fluid domain; the remaining integration over k cannot be performed in closed form and numerical computations must be used.

Now consider a three-dimensional fluid domain, D, with cylindrical coordinates r, z, and θ, bounded above by a free surface, S_f, below by a solid boundary, S_b, and unbounded in the radial direction, i.e., $0 \le r < \infty$. Initially the fluid field is at rest with the free surface and bed located at $z = 0$ and $z = -h$, respectively. For $t > 0$ the bed is permitted to deform in a prescribed manner given by $z = -h + \zeta(r;t)$; hence, only axially symmetric deformations of the bed are considered in this model. The water surface displacement resulting from an axisymmetric bed deformation will also be independent of θ and is given by $z = \eta(r;t)$. Under the same assumptions stated previously for the two-dimensional fluid domain, the linearized description of fluid behavior is given by:

$$\varphi_{rr} + \varphi_r + \varphi_{zz} = 0 \qquad \text{in D,} \qquad (13)$$

$$\varphi_{tt}(r,0;t) + g\varphi_z(r,0;t) = 0 \ , \qquad (14)$$

$$\varphi_z(r,-h;t) = \zeta_t(r;t) \ . \qquad (15)$$

Eqs. (13), (14), and (15) are most easily solved by first using the Hankel transform of zeroth order with respect to the radial coordinate r and the Laplace transform with respect to t. (See Hammack (1972) for the details of this solution.) The resulting water surface displacement is found to be:

$$\eta(r;t) = \int_0^\infty k J_o(kr)\left\{\lim_{\Gamma\to\infty}\frac{1}{2\pi i}\int_{\mu-i\Gamma}^{\mu+i\Gamma}\frac{s^2 e^{st}\tilde{\zeta}(k;s)\, ds}{(s^2+\omega^2)\cosh kh}\right\} dk \ , \qquad (16)$$

where ω^2 is defined by Eq. (8) and the use of the tilda superscript with the bed displacement indicates:

$$\tilde{\zeta}(k;s) = \int_0^\infty dr \int_0^\infty r J_o(kr)\, e^{-st}\zeta(r;t)\, dt \ . \qquad (17)$$

The bracketed quantity in Eq. (16) again represents the complex inversion integral for the Laplace transform of a function while the remaining integration is the inversion integral for the Hankel transform of zeroth order. (The Bessel function of first kind and zero order in Eqs. (16) and (17) is denoted by $J_o(\ )$.)

In order to compare the wave structures resulting from similar bed deformations in the two-dimensional (2-D) and the three-dimensional (3-D) models of tsunami generation, consider a bed deformation for the 3-D model given by:

$$\zeta_e(r;t) = \zeta_o(1-e^{-\alpha t})\, H(r_o - r) \ , \qquad \text{for } t \ge 0 \ , \qquad (18)$$

where H( ) is the Heavyside step function. Eq. (18) represents a bed deformation in which a block section of the bed, circular in planform with a radius r_o, moves with the same time-displacement history as the block section of the bed in the 2-D model; hence, Eqs. (10) and (18) represent analogous bed deformations in the 2-D and 3-D models of tsunami generation, respectively. Three parameters again are required to characterize the bed motion given by Eq. (18): an amplitude, ζ_o, a size, r_o, and a characteristic time, t_c. The characteristic time will again be chosen as the time required for two-thirds of the bed displacement to be completed. Substituting $\zeta_e(r,t)$ as given by Eq. (18) into Eq. (17) yields:

$$\tilde{\zeta}_e(k;s) = \zeta_o \frac{r_o J_1(kr_o)}{k} \left[\frac{\alpha}{s(s+\alpha)}\right] , \qquad (19)$$

where $J_1( )$ is the Bessel function of first kind and order one. Substituting Eq. (19) into Eq. (16), performing the integration around the Bromwich contour, taking only the real part of the results, and noting that the integrand is an even function of k yields:

$$\eta(r;t) = -\zeta_o r_o \int_0^\infty \frac{J_1(kr_o) J_o(kr)}{\cosh kh} \left[\frac{\alpha^2}{\alpha^2+\omega^2}\right]\left[e^{-\alpha t} - \cos \omega t - \frac{\omega}{2} \sin \omega t\right] dk . \qquad (20)$$

The remaining integration over k cannot be performed in closed form and, as with the two-dimensional example, numerical computations must be used to approximate the results.

Eqs. (12) and (20) describe the water surface displacements resulting from similar bed deformations in a two and three-dimensional model of tsunami generation. It should be emphasized that these solutions are based on a linearized description of fluid behavior; hence, their applicability is restricted to bed motions in which the neglected nonlinear effects are small relative to the linear effects which have been retained.

PRESENTATION AND DISCUSSION OF RESULTS

The results presented in this study for the two and three-dimensional models of tsunami generation will be concerned primarily with the wave structure near the source region of the bed deformation. This area of the fluid domain will be referred to as the generation region and is given by $|x| \leq b$ for the 2-D model and $r \leq r_o$ for the 3-D model. Some comments on the propagation of waves outside of the generation region will be presented for the two-dimensional model.

The Generation Region – There are two positions in the generation region of the 2-D model which have been investigated both experimentally and theoretically; these positions are $x/h = 0$ and $x/b = b/h$. (For a discussion of the experimental equipment used to model the bed deformation for the two-dimensional model, see Raichlen (1970) or Hammack (1972).) Analogous positions in the 3-D model (which have been investigated only theoretically) are $r/h = 0$ and $r/h = r_o/h$. The results presented for the positions at the edge of the bed deformation, i.e., $x/h = b/h$ and $r/h = r_o/h$, are of special interest since the wave structure at these locations represents the type of wave which propagates from the source region.

It has been shown by Hammack (1972) that three dimensionless parameters are important in determining the characteristics of the waves in the generation region. These parameters are: ζ_o/h which represents a disturbance-amplitude scale, b/h or r_o/h which represents a disturbance-size scale, and $t_c\sqrt{gh}/b$ or $t_c\sqrt{gh}/r_o$ (hereafter referred to as the time-size ratio) which is the ratio of a disturbance-time scale, $t_c\sqrt{g/h}$, and the disturbance-size scale. The time-size

ratio may also be interpreted as the ratio of a characteristic distance a long wave will propagate during the bed motion to the characteristic length of the bed deformation. When the bed displacement is very rapid such that $t_c\sqrt{gh}/b$ (or $t_c\sqrt{gh}/r_o$) is much less than unity during the displacement interval, the effect of the bed deformation is confined to the neighborhood of the generation region. Bed motions of this type will be referred to as impulsive. When the bed displacement is very slow such that the time-size ratio is much greater than unity, the water surface elevations (depressions) which occur have sufficient time to propagate from the generation region during the displacement interval; hence, the displaced water volume is spread over a larger region of the fluid domain at the end of the bed displacement. Bed motions of this type will be referred to as creeping.

One of the more important characteristics of waves in the generation region is the maximum displacement of the water surface, η_o, which occurs at a particular location. Fig. 2 shows the experimental and theoretical variation at x/h = b/h of the ratio of the maximum wave amplitude, η_o, to the total bed displacement, ζ_o, as a function of the time-size ratio, $t_c\sqrt{gh}/b$. The results are presented separately for each of the five disturbance-size scales (b/h) investigated. Hollow symbols are used to indicate data for which a bed upthrust ($\zeta_o > 0$) occurred; shaded symbols indicate data for bed downthrows ($\zeta_o < 0$). The magnitude of the disturbance-amplitude scale for each experiment is shown in the legend of Fig. 2.

The general behavior of the theoretical variation of the relative wave amplitude, η_o/ζ_o, with the time-size ratio shown in Fig. 2 is similar for each size scale. For impulsive bed motions, i.e., $t_c\sqrt{gh}/b << 1$, the relative wave amplitude reaches a maximum and remains constant with decreasing time-size ratios. The results for impulsive bed motions of the larger size scales indicate that the maximum amplitude of the wave propagating from the generation region is equal to one-half of the total bed displacement; for the smaller size scales the maximum wave amplitude appears to be less than $0.5\,\zeta_o$. As the time-size ratio becomes very large, i.e., for creeping bed motions, the linear theory indicates that the relative wave amplitude becomes inversely proportional to the time-size ratio. (The range of time-size ratios between the impulsive and creeping range will be referred to as transitional.)

The linear theory presented in Fig. 2 for the three smaller size scales agrees well with the variation found from the experiments; however, it should be noted that no disturbance-amplitudes scales, ζ_o/h, greater than 0.2 (in absolute value) were used for these experiments. The experimental results presented for the two larger size scales in Fig. 2 indicate that nonlinear effects become important as the disturbance-amplitude scale exceeds 0.2 when the bed motion is either impulsive or transitional. In the creeping range the linear theory agrees well with the data regardless of the magnitude of ζ_o/h. (This suggested nonlinear behavior in the generation region due to large amplitude scales has been demonstrated analytically by Hammack (1972) for impulsive and creeping bed motions.)

In order to compare the behavior of the relative wave amplitude, η_o/ζ_o, between the two and three-dimensional models of tsunami generation, the theoretical variation of the relative wave amplitude for corresponding time-size ratios has been computed at the center of the disturbance (x/h = 0 and r/h = 0) and at the leading edge (x/h = b/h and r/h = r_o/h) for a size scale of b/h = r_o/h = 12.2. The results presented in Fig. 3 show that at x/h = b/h or r/h = r_o/h the computed variations are similar in shape; an impulsive, transitional, and creeping range of time-size ratios can be defined also for the 3-D model. The relative wave amplitude for the 3-D model is smaller than that

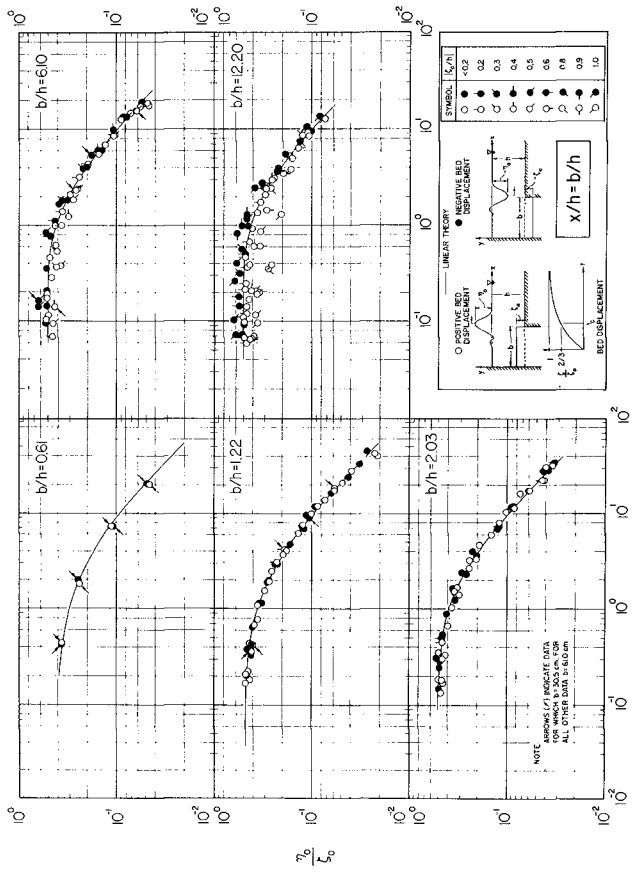

Fig. 2 Variation of the relative maximum wave amplitude, η_o/ζ_o, with the time-size ratio, $t\sqrt{gh}/b$, at $x/h = b/h$ for exponential bed displacements.

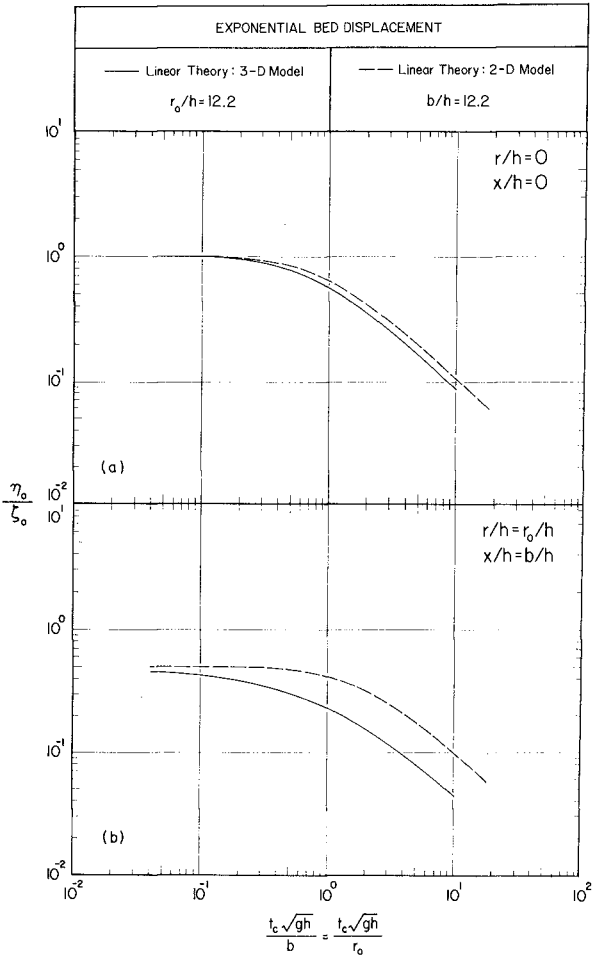

Fig. 3 Theoretical variation of relative maximum wave amplitude, η_o/ζ_o, with the time-size ratio, $t_c\sqrt{gh}/r_o$; a) at $r/h = 0$, b) at $r/h = r_o h$.

computed for the 2-D model over the full range of time-size ratios. At the center of the moving bed, i.e., $x/h = r/h = 0$, the relative wave amplitudes become equal to unity for impulsive bed motions; hence the water surface moves with the bed. In the transitional and creeping range of time-size ratios, the relative wave amplitude is slightly larger for the 2-D model; however, in both cases η_o/ζ_o becomes inversely proportional to the time-size ratio for creeping bed motions.

It was shown in Fig. 2 that the maximum value of the relative wave amplitude in the impulsive range of time-size ratios began to decrease below 0.5 as the disturbance-size scale became very small. This behavior is a result of the elliptic nature ($\nabla^2\varphi = 0$) of the response of the fluid field to an impulsive boundary condition. In order to investigate this behavior more thoroughly for both the two and three-dimensional models, computations of η_o/ζ_o as a function of the disturbance size scales (b/h or r_o/h) for impulsive bed motions have been performed. The results of these computations at the center ($x/h = r/h = 0$) and at the leading edge ($x/h = b/h$ and $r/h = r_o/h$) of the disturbance are shown in Fig. 4; the time-size ratios used for these computations were less than 10^{-2} and 10^{-3} for the two and three-dimensional models, respectively.

The results for the 2-D model indicate that η_o/ζ_o becomes equal to unity and to one-half at $x/h = 0$ and $x/h = b/h$, respectively, for size scales greater than approximately four. For smaller size scales the relative wave amplitude at each position begins to decrease and for $b/h < 10^{-1}$ at each position the relative wave amplitude become equal and directly proportional to the size scale.

For the 3-D model, Fig. 4 shows that η_o/ζ_o becomes equal to unity at $r/h = 0$ for size scales greater than approximately four (similar to the 2-D model); however, at $r/h = r_o/h$ the relative wave amplitude approaches a value of one-half in an asymptotic manner and doesn't become identical to the results of the 2-D model until approximately $r_o/h = 10^2$. For size scales such that $r_o/h < 10^{-1}$ the computations indicate that η_o/ζ_o is equal at both positions in the generation region; η_o/ζ_o also becomes proportional to $(r_o/h)^2$ in this range. Hence, the two and three-dimensional models of tsunami generation behave quite differently for small disturbance-size scales.

In addition to the maximum wave amplitudes, it is also of interest to examine the temporal variation of the water surface movement at a given location in the generation region. Since the temporal behavior of the water surface is similar in each of the three regions: impulsive, transitional, or creeping, it is sufficient to examine typical wave structures for each region. Examples of the theoretical and experimental wave profiles at the center and the leading edge of the bed deformation are presented in Fig. 5 for the 2-D model where the water surface elevation, η, has been normalized by the total bed displacement, ζ_o, and is shown as a function of the nondimensional time $t\sqrt{g/h}$. (The disturbance-size scale, b/h, is equal to 12.2 for each record; a disturbance-amplitude scale, ζ_o/h, has been chosen in each case for which the linear theory is expected to be applicable.)

For the impulsive bed motion shown in Fig. 5, the water level rises rapidly to a maximum elevation of ζ_o and $\zeta_o/2$ at $x/h = 0$ and $x/h = b/h$, respectively, remains at this elevation for an interval of time, and then rapidly returns to the still water level (SWL) about which it oscillates in a damped manner. Most of the wave energy is confined in a single lead wave which resembles the actual bed deformation. The linear theory agrees reasonably

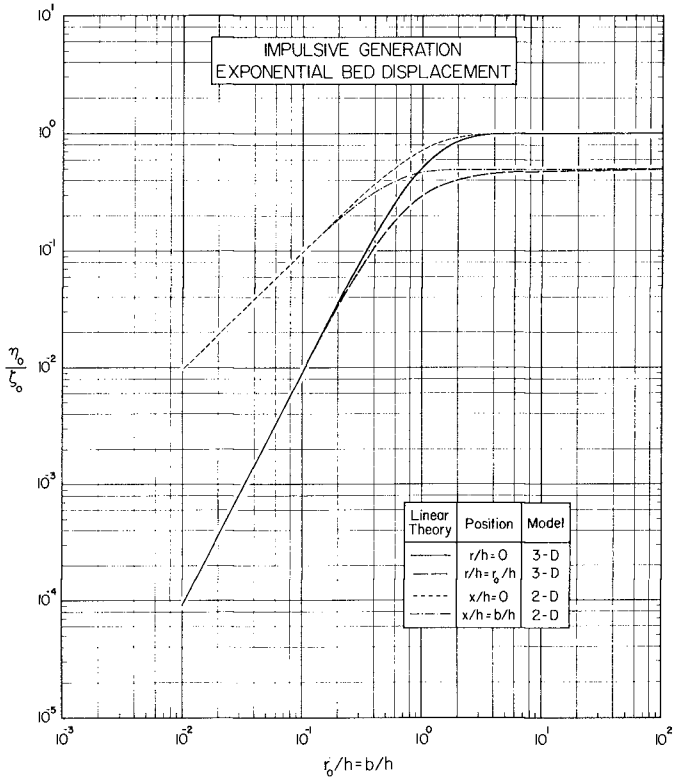

Fig. 4 Theoretical variation of relative maximum wave amplitude, η_o/ζ_o, with the disturbance-size scale, $r_o/h = b/h$, for impulsive bed displacements.

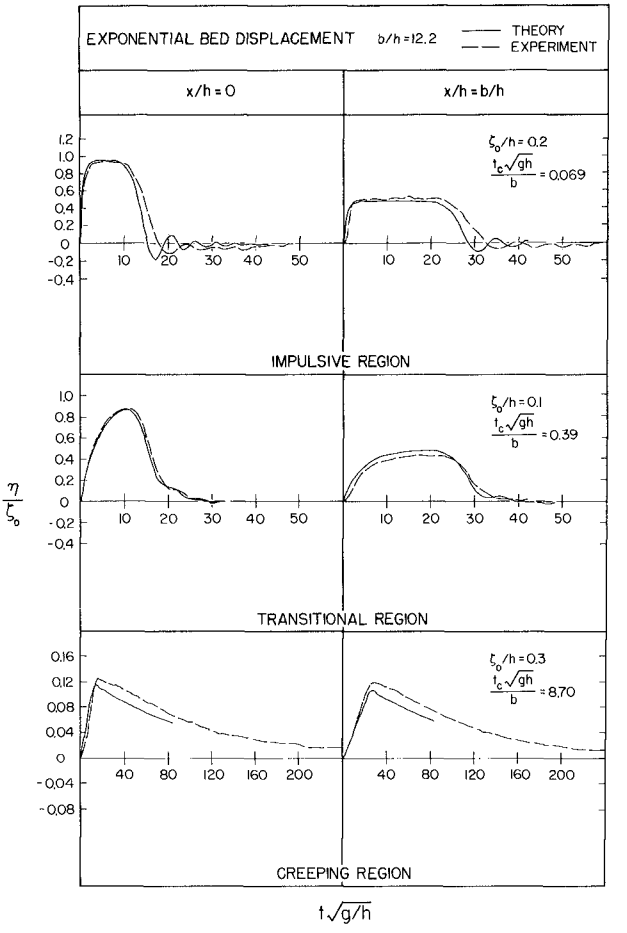

Fig. 5 Typical wave profiles in each region of generation at x/h = 0 and x/h = b/h generated by exponential bed displacements.

well with the measured profile; however, small differences do occur near the trailing portion of the lead wave. The wave profile at $x/h = b/h$ is typical of waves which propagate from the source region of an impulsive upthrust of a block section of the sea bed.

In the transitional and creeping ranges, the water level rises more slowly to a maximum elevation and immediately begins to return to the still water level. The rate of fall of the water level to the SWL for a creeping bed motion is so slow that the wave propagating from the generation region resembles a bore at $x/h = b/h$.

Typical wave profiles generated at the center ($r/h = 0$) and leading edge ($r/h = r_o/h$) of similar bed deformations for the 3-D model are shown in Fig. 6. The wave amplitude, η, again has been normalized by the total bed displacement, ζ_o, and is shown as a function of the nondimensional time, $t\sqrt{g/h}$. A disturbance-size of $r_o/h = 12.2$ has been chosen for each record; hence, a direct comparison is possible with the results presented in Fig. 5 for the 2-D model.

The lead wave at $r/h = 0$ resulting from an impulsive upthrust of the bed resembles that observed for the 2-D model at $x/h = 0$; however, after the water level returns to the SWL it now continues to decrease to a negative elevation of $-1.6\ \zeta_o$. Large amplitude oscillations then occur about a mean level which appears to be approaching the SWL. The positive lead wave that results at $r/h = r_o/h$ is now observed to be followed by a negative wave of comparable amplitude and period; no significant negative waves were observed to result in Fig. 5 from a bed upthrust in the 2-D model.

The positive lead wave resulting from a bed modtion in the transitional region in Fig. 6 is followed by a single negative wave with a larger period and a smaller maximum amplitude than that observed for an impulsive bed motion. When the time-size ratio indicates that the bed motion is creeping, a single positive wave is observed to propagate from the generation region; a similar wave also resulted for a creeping bed motion in the 2-D model.

Tsunami Propagation in a Two-Dimensional Fluid Domain of Uniform Depth. Once a wave propagates from the generation region of the two-dimensional model described in the previous sections, it enters a fluid domain of uniform depth. The linear theory derived in the previous section provides an adequate description of the propagating wave as long as the nonlinear terms which were neglected by this theory remain small compared to the linear terms which have been retained. It is well known that the magnitude of the nonlinear effects (or amplitude dispersion) in a long wave is characterized by the parameter, η_o/h, where η_o is the maximum wave amplitude and h is the water depth. The linear effects (or frequency dispersion) are characterized by $(h/\ell)^2$ where ℓ is a characteristic length of the wave. Hence, the relative importance of nonlinear effects is indicated by the ratio:

$$\underline{U} = \frac{\eta_o/h}{(h/\ell)^2} = \frac{\eta_o \ell^2}{h^3} \quad , \tag{21}$$

which will hereafter be referred to as the Ursell Number although Korteweg and de Vries (1875) as well as Ursell (1954) discussed the significance of this parameter in characterizing long wave propagation. When the Ursell Number is much less than unity for a wave, the linear theory provides an adequate description of wave behavior. When the Ursell Number is much greater than unity, the linear effect of frequency dispersion may be neglected and only the nonlinear effect of amplitude dispersion need be considered in approximating

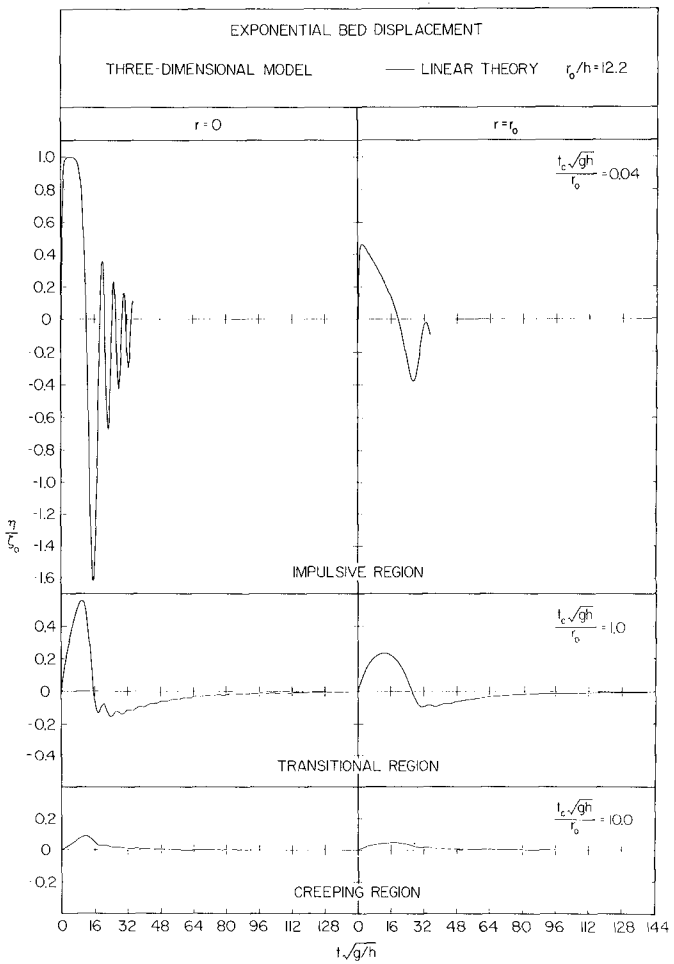

Fig. 6 Typical wave profiles in each region of generation at $r/h = 0$ and $r/h = r_o/h$ generated by exponential bed displacements.

the wave behavior. For the special case of small-but-finite non-linear effects such that η_o/h is of the order of $[(h/\ell)^2]$, a theory which describes the wave behavior must retain both amplitude and frequency dispersion effects; approximate theories such as those developed by Boussinesq (1872) or Korteweg and deVries (1895) provide an adequate description of wave behavior for this special case. It is well known that waves of permanent form (the solitary or cnoidal waves) exist for this special case, i.e., when the Ursell Number is about unity. These permanent form waves result as a balance between the competing effects of amplitude and frequency dispersion is achieved.

Ursell (1954) showed that nonlinear effects grow like $t^{\frac{1}{3}}$ for a long wave propagating in a two-dimensional fluid domain which is initially described by a linear theory (see Hammack (1972) for a more detailed discussion of this). Hence, the linear theory presented in the previous section will eventually become inadequate as a description of wave behavior and a theory such as that of Korteweg and deVries (KdV), which considers both amplitude and frequency dispersion (in an approximate manner), would appear to be required to describe the wave behavior.

The equation of Korteweg and deVries has been the subject of extensive research recently due to the discovery by Gardner et al (1967) of an exact solution algorithim for this equation with arbitrary initial conditions. The exact solution indicates that a finite number of solitary waves (or solitons) will emerge from an initial wave form; these solitons are ordered by decreasing amplitude toward the rear of the train and are followed by a dispersive train of oscillatory waves. Zabusky (1968) and Segur (1972) have shown that this pattern of wave behavior evolves when the initial wave contains a net positive volume. The Ursell Number for this train of solitary waves remains constant during further propagation, since these waves are permanent in form and the competing effects of amplitude and frequency dispersion are balanced.

These properties of the solution of the KdV equation for an initial wave $\int_{-\infty}^{\infty} \eta(x;\sigma)dx > 0$, i.e., the net wave volume is positive, suggest the following procedure for developing a uniformly valid solution of the wave behavior resulting from a bed upthrust for which a linear theory initially provides an adequate description of wave behavior, i.e., $U << 1$ near the generation region. The linear theory may be used to determine the wave behavior until the Ursell Number, computed in an appropriate manner, indicates that nonlinearities are becoming important; the wave profile computed using the linear theory can then be used as an initial condition for the KdV equation which may be solved to determine further wave behavior for all time. An example of this strategy will be presented shortly .

In order to apply the suggested strategy the Ursell Number must be evaluated for a variety of complex (non-sinusoidal) wave profiles in a reasonable way to indicate when frequency and amplitude dispersion are about equal. No single length may exist which adequately describes a complex wave; hence, the Ursell Number becomes a variable parameter in different regions of the wave. An appropriate definition of the length, ℓ, in a region of a complex wave is $\ell = 0\,(\eta/\eta_x)$ where η_x represents the slope of the wave. In order to determine a numerical value for ℓ, the following operational definition may be used:

$$\ell = |\eta_o| / |(\eta_x)_{max}| \,, \tag{22}$$

where $|\eta_o|$ is the absolute value of the total change in wave elevation within the region and $|(\eta_x)_{max}|$ is the absolute value of the maximum slope of the water surface in the region. Hence, the Ursell Number becomes:

$$\underline{U} = \frac{\eta_o |\eta_o|^2}{h^3 |(\eta_x)_{max}|^2} \quad . \tag{23}$$

An appropriate region of a complex wave can then be defined as the region between two successive positions of zero wave slope ($\eta_x = 0$). When Eq. (23) is applied to each region of a solitary wave, the Ursell Number is found to be approximately two; hence, an Ursell Number of about two when computed by Eq. (23) should indicate that frequency and amplitude dispersion are about equal. (It should be noted that the Ursell Number in the leading region of a complex wave will normally be the largest for the wave since the longest wave components travel the fastest.)

Due to the complexity of the method for the exact solution of the KdV equation, a numerical solution algorithim has been adopted. The numerical solution is similar to that introduced by Peregrine (1966) and is based on an equation of the KdV type in the form:

$$u_t + (1 + \frac{3}{2}u)\, u_x - \frac{1}{6} u_{xxt} = 0 \quad , \tag{24}$$

where us is a nondimensional velocity ($u = u^*/\sqrt{gh}$), x is a nondimensional space coordinate ($x = x^*/h$) and t is a nondimensional time ($t = t^*\sqrt{g/h}$). The velocity u, is related to the wave amplitude, η, to the same order of approximation, by:

$$\eta = u + \frac{1}{4}u^2 - \frac{1}{6} u_{xx} \quad . \tag{25}$$

A simple finite-difference approximation of Eq. (24) was found to be stable by Peregrine. The accuracy of this finite-difference approximation for a specific grid size is easily determined by propagating a solitary wave numerically; changes of the shape of this wave during propagation are due to the approximation. The accuracy of the finite difference model can be improved by decreasing the grid size.

In order to illustrate the suggested strategy for a bed upthrust, an experiment with the following generation parameters has been investigated:

$$\zeta_o/h = 0.1, \quad b/h = 12.2, \quad t_c\sqrt{gh/b} = 0.148 \quad . \tag{26}$$

From the previous discussion, a linear theory would be expected to accurately describe the waves near the generation region for the parameters of Eq. (26). Fig. 7a shows the measured wave profiles at the leading edge of the bed section, $(x-b)/h = 0$, and at three more positions downstream: $(x-b)/h = 20$, 180, and 400. The wave amplitude, η, has been normalized by the water depth and plotted as a function of the nondimensional time: $t\sqrt{g/h} - (x-b)/h$.

The measured wave observed to be leaving the generation region at $(x-b)/h = 0$ resembles the actual bed deformation. During propagation the single lead wave appears to separate into three individual waves (or solitons) and a dispersive wave train develops behind these leading solitons. The Ursell Number as calculated by Eq. (23) is indicated in Fig. 7a for the frontal region of the lead wave. At only twenty depths the Ursell Number is equal to 0.7; hence, frequency dispersion is only slightly larger than amplitude dispersion. At $(x-b)/h = 180$ and 400 the Ursell Number is two and three, respectively; thus, frequency and amplitude dispersion effects are about equal. (Only one significant digit for the Ursell Number is indicated in Fig. 7.)

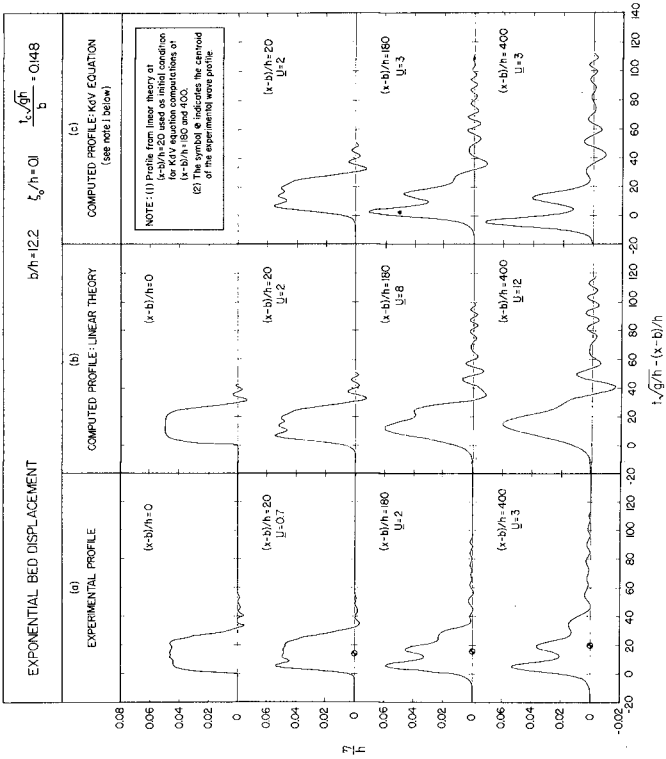

Fig. 7 Downstream wave profiles generated by an impulsive exponential bed upthrust; a) measured, b) computed by linear theory, c) computed by KdV equation.

Fig. 7b shows the wave profiles at each downstream position as computed by the linear theory, i.e., Eq. (12). The computed profiles at $(x-b)/h = 0$ and $(x-b)/h = 20$ agree well with the measured profiles in Fig. 7a; however, at the downstream positions of $(x-b)/h = 180$ and 400 the linear theory no longer predicts the measured wave structure well. Frequency dispersion, unhindered by amplitude dispersion in the linear theory, continues to disperse the wave into its spectral components. The continual growth of the Ursell Number in the front region of the lead wave from $\underline{U} = 2$ at $(x-b)/h = 20$ to $\underline{U} = 12$ at $(x-b)/h = 400$ is a result of this frequency separation.

Following the suggested strategy for determining wave behavior after nonlinear effects have become important, the linear theory at $(x-b)/h = 20$ (where $\underline{U} = 2$) has been used as the initial condition for Eq. (24). The profiles computed by this equation at $(x-b)/h = 180$ and 400 are shown in Fig. 7c. The temporal variation of these profiles agree well with the measured results in Fig. 7a. The Ursell Number for the front region of the lead wave in Fig. 7c remains constant at a value of three; hence, frequency and amplitude dispersion are of the same order during wave propagation and solitons are emerging.

The difference between measured and computed wave amplitudes in Fig. 7a and Fig. 7c are the result of viscous effects in the experimental model. Corrections applied to the experiments for these viscous effects (see Hammack, (1972)) indicate that Eq. (24) does predict these amplitudes well for a non-dissipative fluid medium.

Oscillating Bed Motions With a Mean Displacement - In the preceding sections only a simple time-displacement history of the bed motion was considered. In order to observe experimentally the effect of a more general time-displacement history on the resulting waves, experiments were conducted where an oscillating motion (or dither) was superposed on the mean displacement; the frequency and amplitude of this dither was varied. Fig. 8 abc shows the measured waves in the generation and downstream region resulting from three bed displacements with the same mean motion; the wave amplitude, η, has again been normalized by the water depth, h, and shown as a function of the nondimensional time $t\sqrt{g/h} - (x-b)/h$. The actual time-displacement history of the bed section is also shown in Fig. 8.

Waves resulting from the mean motion alone are shown in Fig. 8a. Note that this mean motion (termed the half-sine bed displacement) occurs in a finite time, t_c; the generation parameters for this motion are:

$$\zeta_o/h = 0.2, \quad b/h = 12.2, \quad t_c\sqrt{gh}/b = 1.10 \ . \tag{27}$$

The time-size ratio in Eq. (27) indicates that this bed displacement is near the boundary between the impulsive and transitional ranges of time-size ratios (see Hammack, 1972 for more details of this mean motion). The wave measurements in Fig. 8a for the mean motion again demonstrate the evolution of solitons from the positive lead wave which propages from the generation region. In Fig. 8b a dither is superposed on the mean motion with a period, τ, of one-half the characteristic time, t_c, of the mean motion and an amplitude, ζ_1, of one-half the total bed displacement. The lead region of the wave profiles in the generation region $(x-b)/h = -b/h$ and 0 resemble the actual bed displacement; the wave leaving the generation region at $(x-b)/h = 0$ contains several small oscillatory waves superposed on the larger wave which are apparently created by the mean motion alone. These oscillatory waves are left behind by the mean wave during propagation until, at $(x-b)/h = 400$, the measured wave resulting from this bed motion is almost identical to the results for the mean bed displacement alone in Fig. 8a.

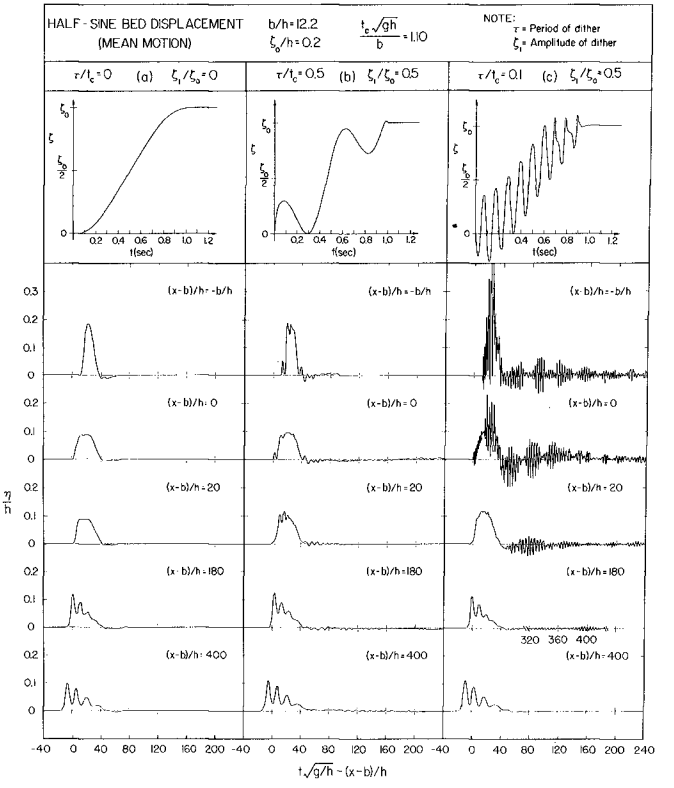

Fig. 8 Measured wave profiles; a) an impulsive half-sine mean motion, b), c) half-sine mean motion with a superposed oscillation.

Fig. 8c shows the waves generated when the period, τ, of the superposed dither is reduced to $0.1\ t_c$ while the amplitude, ζ_1, is maint ined at $0.5\ \zeta_o$. Large amplitude cross waves, i.e., waves propagating laterally across the wave tank, were created in the generation region by this bed motion. These cross waves also created high frequency oscillatory waves that propagated downstream as evidenced by the measurements at $(x-b)/h = 20$ and 180. These oscillatory waves appear to decay very rapidly (due to the combined effect of frequency separation and viscosity) and are again left behind by a large wave which is apparently created by the mean motion of the bed only. The measured wave at $(x-b)/h = 400$ is almost identical to the results found in Fig. 8a; hence, it appears that the detailed time-displacement history for an impulsive bed motion may not be of critical importance in determining the wave behavior downstream of the generation region. (It should be noted that the opposite was found to be true by Hammack (1972) for creeping mean motions with a superposed dither. A knowledge of the exact time-displacement history of the bed section is of major importance in determining the downstream wave behavior when the mean motion is creeping.)

CONCLUSIONS

The following conclusions regarding tsunami generation and propagation can be drawn from the theoretical and experimental models investigated in this study:

1) The maximum amplitude of the wave propagating from the generation region is approximately one-half of the total bed displacement for both the two and three-dimensional models of tsunami generation which were studied.

2) The linear theory appears to accurately predict the wave structure in the generation region whenever the disturbance-amplitude scale, ζ_o/h, is less than 0.2 in absolute value.

3) Major differences exist between the structure of the wave propagating from the generation region of the 2-D and 3-D models investigated; large negative waves can result from an impulsive bed uplift in the 3-D model while no large negative waves result from a bed uplift in the 2-D model.

4) Nonlinear effects grow during wave propagation in the 2-D model so that the linear theory eventually becomes an inadequate description of wave behavior; an equation similar to that of Korteweg and deVries was shown to be the proper model of wave behavior once linear and nonlinear effects become about equal.

5) A detailed knowledge of the time-displacement history of an impulsive bed motion may be unimportant in determining the wave behavior outside of the generation region.

ACKNOWLEDGMENT

This study was supported by the National Science Foundation under Grants GK-2370 and GK-24716 and was conducted at the W. M. Keck Laboratory of Hydraulics and Water Resources, California Institute of Technology.

LIST OF REFERENCES

Boussinesq, J. 1872 "Theorie des ondes et des remous qui se propagent le long d'un canal rectangulaire horizontal, en communiquant au liquide contenu dans ce canal des vitesses sensibilement pareilles de la surface au fond", J. de Mathematiques Pures et Appliquees, 2nd Serie, 17, 55-108.

Gardner, C.S., Greene, J.M., Kruskal, M.D., and Miura, R.M. 1967 "Method for Solving the Korteweg-deVries Equation", Phys. Rev. Ltrs, 19, 1095-1097.

Hammack, J. L., Jr., 1972 "Tsunamis - A Model of Their Generation and Propagation", Rep. No. KH-R-28, W.M. Keck Lab. of Hydraulics & Water Resources, California Institute of Technology.

Honda, H., and Nakamura, K., 1951, "The Waves Caused by One-Dimensional Deformation of the Bottom of Shallow Sea of Uniform Depth", Science Report Tohoku University, Sendai, Japan, 3, 133-137.

Hwang, L.S., and Divoky, D., 1970, "Tsunami Generation", JGR, 75, 6802-6817.

Ichiye, T., 1950, "On the Theory of Tsunami", Ocenographical Magazine, 2, 83-100.

Kajiura, K., 1963, "The Leading Wave of a Tsunami", Bull., Earthquake Research Institute, Tokyo University, 41, 535-571.

Keller, J.B., 1963, "Tsunamis - Water Waves Produced by Earthquakes", Intern. Union of Geodesy & Geophysics, Monograph No. 24, 154-166.

Korteweg, D. J., and deVries, G., 1895, "On the Change of Form of Long Waves Advancing in a Rectangular Canal, and on a New Type of Long Stationary Waves", London, Edinburgh, and Dublin Philosophical Mag., Ser. 5, 39, 422-443.

Momoi, T., 1964, "Tsunami in the Vicinity of a Wave Origin", Bull. Earthquake Research Institute, Tokyo University, 42, 133-146.

Nakamura, K., 1953, "On the Waves Caused by the Deformation of the Bottom of the Sea, I", Science Report, Tohoku University, Sendai, Japan, 5th Series, 5, 167-176.

Peregrine, D.H., 1966, "Calculations of the Development of an Undular Bore", J. Fluid Mech., 25, 321-330.

Raichlen, F., 1970, "Tsunamis: Some Laboratory and Field Observations", Proc. 12th Coastal Engineering Conf., Washington, D.C., 2103-2122.

Segur, H., 1972, "The Korteweg-deVries Equation and Water Waves. I. Solution of the Equation", submitted to the J. Fluid Mechanics.

Takahashi,R. 1942, "On Seismic Sea Waves Caused by Deformations of the Sea Bottom", Bull. Earthquake Research Institute, Tokyo University, 20, 275-400.

Takahashi, R., 1945, "On Seismic Sea Waves Caused by Deformations of the Sea Bottom, 2nd Report", Bull. Earthquake Research Inst., Tokyo Univ., 23, 23-35, (in Japanese).

Takahashi, R., 1947, "On the Seismic Sea Waves Caused by Deformations of the Sea Bottom, 3rd Report", Bull. Earthquake Res. Inst., Tokyo Univ., 25, 5-8.

Takahasi, R., 1963, "On Some Model Experiments on Tsunami Generation", Intern. Union of Geodesy & Geophysics, Monograph No. 24, 235-248.

Takahasi, R., and Hatori, T., 1962, "A Model Experiment on the Tsunami Generation from a Bottom Deformation Area of Elliptic Shape", Bull. Earthquake Research Institute, Tokyo University, 40, 873-883.

Ursell, F., 1953, "The Long-Wave Paradox in the Theory of Gravity Waves", Proc., Cambridge Philosophical Soc., 49, 685-694.

Webb, L. M., 1962, "Theory of Waves Generated by Surface and Sea-Bed Disturbances", Appendix 1, "The Nature of Tsunamis, Their Generation and Dispersion in Water of Finite Depth," Tech. Rep. SN 57-2, Natl, Engrg. Sci. Co.

Zabusky, N. J., 1968, "Solitons and Bound States of the Time-Independent Schrodinger Equation", Phys. Rev., 168, 124-128.